communications earth & environment

ARTICLE

https://doi.org/10.1038/s43247-022-00400-1 OPEN

Black carbon emissions from traffic contribute substantially to air pollution in Nairobi, Kenya

Leonard Kirago [1], Michael J. Gatari [2], Örjan Gustafsson [1] & August Andersson [1✉]

Rapid urbanization and population growth drives increased air pollution across Sub-Saharan Africa with serious implications for human health, yet pollutant sources are poorly constrained. Here, we analyse fine particulate aerosol concentrations and radiocarbon composition of black carbon over a full annual cycle in Nairobi, Kenya. We find that particle concentrations exceed the World Health Organisation's recommended safe limit throughout the year, with little seasonal variability in particle concentration or composition. Organics (49 ± 7%) and water-soluble inorganic ions, dominated by sulfates (13 ± 5%), constitute the largest contributors to the particle loadings. Unlike large cities on other continents, the fraction of black carbon in particles is high (15 ± 4%) suggesting black carbon is a prominent air pollutant in Nairobi. Radiocarbon-based source quantification indicates that fossil fuel combustion emissions are a dominant source of black carbon throughout the year (85 ± 3%). Taken together, this indicates that black carbon emissions from traffic are a key stressor for air quality in Nairobi.

[1] Department of Environmental Science, and the Bolin Centre for Climate Research, Stockholm University, Stockholm 10691, Sweden. [2] Institute of Nuclear Science & Technology, College of Architecture and Engineering, University of Nairobi, Nairobi 30197-00100, Kenya. ✉email: August.Andersson@aces.su.se

Air pollution is the main environmental health hazard worldwide[1,2]. For Africa, around one million premature deaths/year are associated with ambient air pollution, making it more deadly than major diseases like diarrhoea, HIV or malaria[2–5]. Rapid and unplanned urbanisation, characterised by inadequate support infrastructure and policies, contribute to increasing air pollution levels in sub-Saharan Africa (SSA) cities[6–9]. The SSA cities are growing at an annual average rate of 4.2% compared to a global average of 1.7%, and the urban SSA population is thereby projected to double by the year 2040[10]. This calls for effective pollution control measures and policies to address the air quality challenges in the region, in order to reduce the health burden and ensure sustainable urbanisation.

Despite the strong impact on human health and regional climate, air pollution in SSA remains understudied[9,11,12]. The number of observation sites are few, and measurements are typically conducted only in short campaigns, while long-term, year-round observations are central for estimating health and environmental impact[13–16]. Meanwhile, the available data show high pollution levels and an increasing temporal trend[7,17–22]. Projections suggest that anthropogenic emissions in SSA will increase drastically over the coming decades[7,23]. This signifies a major risk to human respiratory health and regional climate, hence the need to combat air pollution. For instance, high exposure to $PM_{2.5}$ and black carbon in Nairobi is an eminent public health risk[16,22,24]. Efforts to address air pollution challenges are however hindered by limited understanding of the relative contribution from different emission sources[16,25,26].

Black Carbon (BC), a primary aerosol from fossil fuel combustion and biomass burning, is one of the more toxic species in $PM_{2.5}$ and a potent climate warmer[27–29]. The sources of BC are poorly constrained in general, but more so in the SSA region due to limited observational data[7,9,23,30]. Chemical transport and climate models, as well as mitigation efforts, largely rely on bottom-up emission estimates in evaluating environmental effects. These estimates typically report large uncertainties, reflecting both activity estimates (fuel consumption data) but perhaps mainly emission factor estimates—emission per unit fuel combusted[31–33]. The activity estimates for SSA are comparably ill-constrained, and it is not generally clear that emission factors typically developed for other regions apply equally well to SSA[7,23,30,34]. Taken together, the uncertainties in estimates of bottom-up emissions are particularly large for SSA.

An alternative, or complement to bottom-up source-segregated emission estimates, is source quantification from source-diagnostic measurements in the ambient atmosphere. For BC, radiocarbon (^{14}C) analysis has proven a particularly effective tracer for differentiating between fossil and biomass burning sources[25,26,32,35]. BC from fossil emissions is completely depleted in ^{14}C ($\Delta^{14}C_{fossil} = -1000‰$), whereas biomass sources have a distinct $\Delta^{14}C$ signature relative to atmospheric CO_2 at the time of carbon fixation ($\Delta^{14}C_{biomass} \approx +50$ ‰, see discussion below)[36]. The ^{14}C signature is determined specifically on BC isolates, and thus do not share the potential ambiguity of other chemical source tracers, which typically have different atmospheric fate, and are actually not parts of the BC pool. In addition, since BC is recalcitrant to physical and chemical transformations, it is not influenced by atmospheric processes and maintains its original ^{14}C isotopic composition[37]. Therefore, the two source categories - fraction fossil and fraction biomass burning—can be differentiated at high precision. This technique has been applied for BC source apportionment in remote regions[38,39] and heavily polluted cities[40,41], yet so far not for the SSA region.

Here, we apply the radiocarbon technique to quantify the sources of BC in SSA. Our study site is located in Nairobi, which is one of the largest and most rapidly growing cities in SSA. Year-round (March 2014 to February 2015) $PM_{2.5}$ filter samples were collected at an urban background site. Together with BC data, we present other $PM_{2.5}$ components; water-soluble inorganic ions and organic carbon (OC) concentrations. The $\Delta^{14}C$ signatures for BC allow us to quantify the relative contribution of biomass burning versus fossil sources, and assess how the sources vary seasonally.

Results and discussion

Meteorology and fires. The meteorology of Nairobi is governed by the East African monsoon system, with major (March to May) and minor (October and November) wet seasons and intersecting dry periods[42]. Overall, there is a limited seasonality in different meteorology parameters during the study period. For instance, comparably scanty rainfall was recorded even during the typical wet seasons, while winds were predominantly north-easterly (SI Fig. S3). On the other hand, the BT analyses show apparent seasonal shifts in air mass origin as a function of the annual oscillation of the inter-tropical convergence zone (ITCZ, Fig. 1). During Boreal winter, the air masses are largely of north-eastern origin, while south-easterly (SE) air masses are intercepted between March and November.

The dry African monsoon periods are associated with large-scale savannah and forest fires, clearly observable from space (Fig. 1). These fires mainly occur north of the equator (e.g. South Sudan, the Central African Republic and Cameroon) between December to February, while the fire regime shifts to the south during the Boreal summer dry period. Even though the majority and more intense fires during Boreal summer occur on the African south-west coast, in D.R. Congo and Angola, considerable fires also occur in Nairobi's upwind, Madagascar and Tanzania (Fig. 1). Given the air mass transport pathways, the fires in these East African countries may influence the aerosol regime in Nairobi through long-range transport, while the analogous phenomenon during the Boreal winter dry period is less likely, as the fires occur downwind.

$PM_{2.5}$ composition. During the present year-round campaign, fine particulate air pollution ($PM_{2.5}$) in Nairobi was found to be continuously elevated, with an annual average of $27 \pm 6\ \mu g\ m^{-3}$. This is five times higher than 2021 WHO recommended annual mean $PM_{2.5}$ guideline value at $5\ \mu g\ m^{-3}$ while surpassing the WHO 24-h limit of $15\ \mu g\ m^{-3}$ in all sampling days[43]. Overall, limited seasonal $PM_{2.5}$ variability was observed in Nairobi, with slightly elevated values during the dry period (Fig. 2 and Table 1), and in agreement with a previous study[18]. No clear links between the observed concentrations and specific meteorological parameters, e.g. estimated PBL height and precipitation, were found. This suggests that variability in these meteorological parameters were not strong enough to impact the urban background aerosol loadings significantly, while atmospheric processing and emissions also modulate the loadings (SI Fig. S3). The largest component of $PM_{2.5}$ was carbonaceous aerosols (CA; $64 \pm 11\%$) with organic aerosols ($OA = 2.1 \times OC$[44]) contributing $49 \pm 7\%$ of the $PM_{2.5}$ loadings, while BC accounts for $15 \pm 4\%$.

The contribution of water-soluble inorganic ions (WSII) amounted to $13 \pm 5\%$ of the $PM_{2.5}$ loadings and was dominated by SO_4^{2-} ($1.8 \pm 0.8\ \mu g\ m^{-3}$; $7 \pm 3\%$). Overall, a larger seasonality was observed in WSII components compared to carbonaceous aerosols, and elevated WSII concentrations were observed during the dry periods, likely attributable to prevailing meteorology and emissions variability, e.g. long-range transport from downwind fires (SI Fig. S1). Besides CA and WSII, $25 \pm 5\%$ of the $PM_{2.5}$ remained unaccounted for, likely reflecting aerosol-bound water and elemental components.

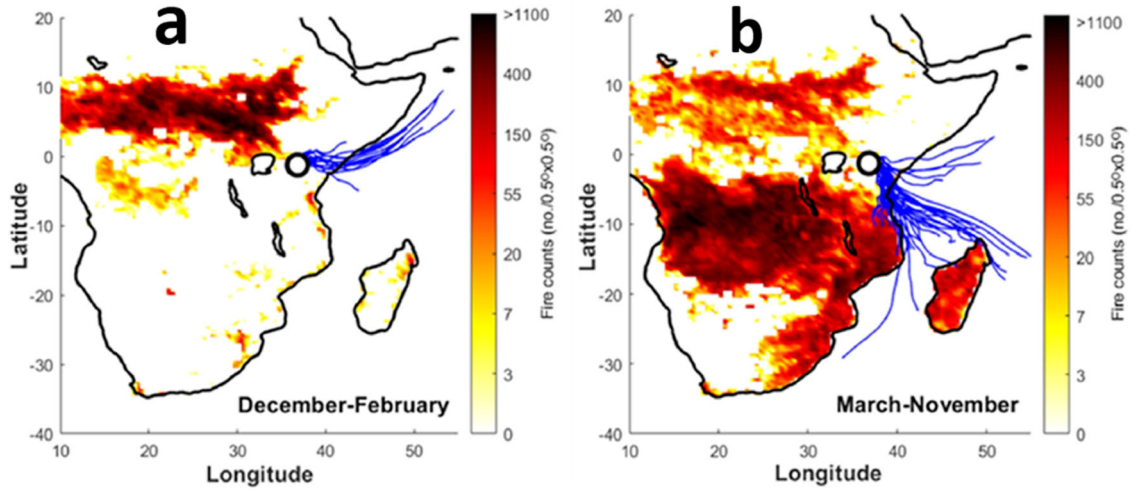

Fig. 1 Fire regimes and airmass back trajectories (BTs, blue lines) during the sampling campaign in Nairobi (white circle with a black outline). a During the December-February period, BTs arriving at Nairobi are mainly from the northeast sector. Meanwhile, large-scale fires mainly occur downwind, with little expected influence on $PM_{2.5}$ composition in Nairobi. **b**. During March-November, the fire regime has largely shifted to the south. During this period, BTs arriving at Nairobi partially overlap with the fires, suggesting a potential impact on the air quality. The fire data were derived from the NASA Moderate Resolution Imaging Spectroradiometer (MODIS) satellite product for March 2014 to February 2015 sampling period. The 5-days air mass BTs were computed every 6 h, with an arrival height of 100 m above ground level (1890 m a.s.l).

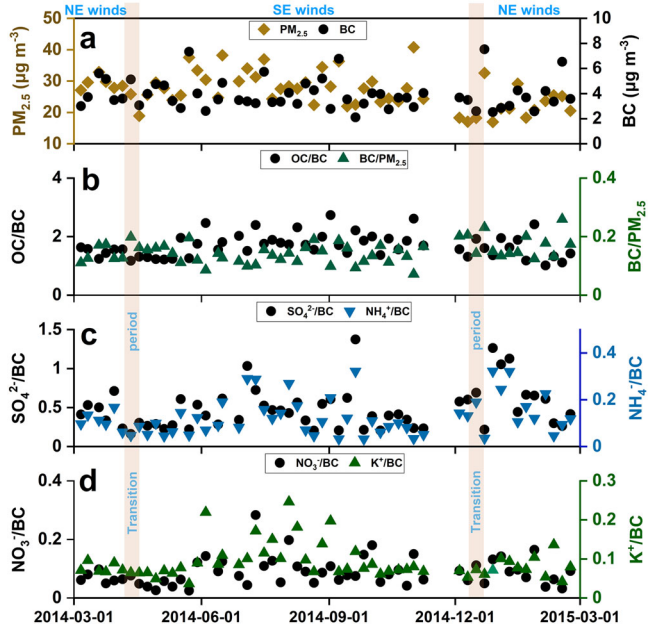

Fig. 2 Year-round variation of $PM_{2.5}$, BC, and source-diagnostic ratios. **a** Shows $PM_{2.5}$ and BC concentrations, **b** shows OC/BC and BC/$PM_{2.5}$ ratios, **c** shows SO_4^{2-}/BC and NH_4^+/BC ratios and **d** presents K^+/BC and NO_3^-/BC ratios. The predominant air masses arriving at Nairobi are marked out on top, and the transition periods are highlighted in light brown colour.

The sea-salt contribution to WSII was estimated to be less than 2%, using Na^+-based estimates, while Na^+ correlated well with Mg^{2+} ($R^2 = 0.79$, $p < 0.01$), another tracer for sea salt (SI Note S2). SO_4^{2-} and NH_4^+ generally have different emissions source profiles but tend to form a stable salt, and are often found to be well correlated[45]. Here, a strong linear relation between SO_4^{2-} and NH_4^+ ($R^2 = 0.75$, $p < 0.01$, and $R^2 = 0.84$, $p < 0.01$ on removing a single outlier), and a molar slope of NH_4^+ vs SO_4^{2-} at 2.2, suggest the formation of $(NH_4)_2SO_4$. Overall, the $PM_{2.5}$ concentration and composition compare well with previously reported urban background values in other SSA cities (SI Table S1).

Table 1 Seasonally averaged $PM_{2.5}$ and BC concentrations (μg m^{-3}), $\Delta^{14}C_{BC}$ signatures (‰) and fraction fossil contribution (f_{fossil}), shown with mean and standard deviation, for the year-round campaign in Nairobi.

	Spring 2014	Summer 2014	Fall 2014	Winter 2014/15
$PM_{2.5}$	28 ± 4	30 ± 5	28 ± 8	22 ± 4
BC	4.2 ± 1.2	3.9 ± 0.9	3.6 ± 1.2	3.9 ± 1.5
$\Delta^{14}C_{BC}$	−861 ± 22	−829 ± 27	−826 ± 48	−837 ± 31
f_{fossil}	0.87 ± 0.02	0.87 ± 0.02	0.86 ± 0.02	0.85 ± 0.02

Black carbon concentrations. The BC levels at the urban background site in Nairobi were steadily high at 3.9 ± 1.2 μg m^{-3}, through the year-round study period (Fig. 2). Similarly to $PM_{2.5}$, no distinct seasonal trend was found for BC. The observed annual mean, and lack of seasonality, is comparable to previously reported values in a two-year study at the same sampling location (May 2008–April 2010; 3.9 ± 0.8 μg m^{-3})[18], and measurements at an industrial background site in the city (a range of 2.3–7.8 μg m^{-3})[46]. However, these background values are much lower than the BC exposure levels reported at the curbsides and bus termini inside the city of Nairobi, which were found above 20 μg m^{-3} and accounted for over 30% of $PM_{2.5}$ mass, as pointed out in the Nairobi City County air quality action plan and reference therein[22,47–49]. The persistently high BC concentrations thus pose a health risk to the over four million city residents.

The BC concentrations in Nairobi are comparable to reported levels in other SSA cities (Fig. 3; SI Table S1). Urban background levels above 3 μg m^{-3} are recorded in different cities across the region, based on the available shorter-term studies[17–22,46,50,51]. Although direct comparisons between cities are complicated by, e.g. intra-city variability and meteorology, the observed BC levels are comparable to those reported in urban background environments in megacities in South and East Asia, but higher than in European and North American cities (Fig. 3 and SI Tables S2, S3). While absolute concentrations are key for exposure and effects, ratios are less dependent on meteorological parameters such as PBL height and ventilation, and thus offer a more conserved

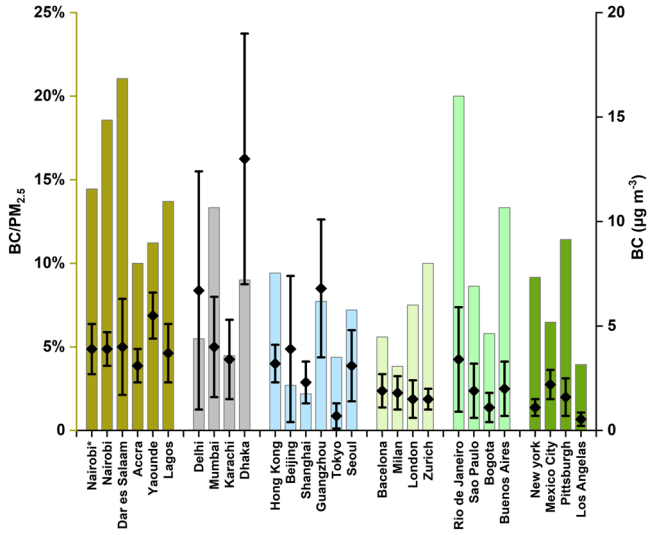

Fig. 3 Comparison of BC/$PM_{2.5}$ ratio (columns; %) and the corresponding BC concentrations (diamonds, with error bar as the standard deviation) reported in major cities globally. Different colours/shades are used to represent cities in different regions for ease of comparison. Nairobi* refers to this study. A detailed compilation and references are provided in SI Table S2.

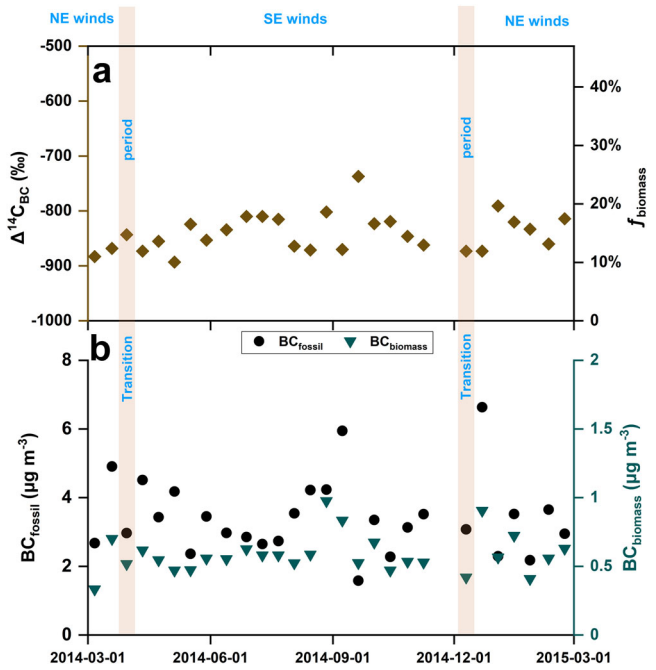

Fig. 4 Year-round variations in BC source contribution in Nairobi. **a** Presents the $\Delta^{14}C$ signatures of BC ($\Delta^{14}C_{BC}$) and the corresponding fractional contribution of biomass burning ($f_{biomass}$), and **b** shows the $\Delta^{14}C$ resolved fossil vs biomass sourced BC concentrations in Nairobi. $\Delta^{14}C$ of −1000‰ implies 100% fossil. Roughly every second sample was analyzed for ^{14}C signatures. The prevailing are masses received in Nairobi, and the transition periods are indicated.

means for comparing pollution characteristics at urban background locations in different cities. For the herein investigated cities, we observe that the BC/$PM_{2.5}$ ratio in Nairobi and other SSA cities are in general elevated (~15%) compared to other global cities, suggesting a unique urban pollution regime and aerosol composition in the region (Fig. 3). Or in other words, the ambient BC pollution is particularly severe in SSA urban environments, which is aggravated by the fact that BC is a particularly toxic $PM_{2.5}$ component.

Source marker ratios. The ratios and correlations between different $PM_{2.5}$ species can give insights into sources and trends. BC and OC are co-emitted from incomplete combustion but at varying emission factors for each, between different sources. Therefore, the OC/BC ratio has sometimes been used as a source-diagnostic marker, where elevated ratios often are interpreted as biomass-influenced regimes[15]. However, OC is also formed from secondary sources and is less recalcitrant than BC in the atmosphere, making OC/BC a non-conservative source tracer[52,53]. In this study, the OC/BC ratio range from 1.0 to 2.7 with little seasonal variability, and partially disparate origins, qualitatively indicating comparably low biomass burning contributions (Fig. 2 and SI Fig. S2).

Additionally, ratios of certain inorganic species may also be indicative of different emission sources. For instance, K^+/EC ratio can be used as a wood/biomass burning marker. Here, we observed elevated K^+/EC ratios during the dry boreal summer period, coinciding with the arrival of air masses through savanna-burning dominated regions in the south and post-harvest season (Fig. 2 and SI Fig. S2). Meanwhile, the NO_3^-/EC is often used as a tracer for traffic emissions and lightning strikes. However, recent studies suggest highly elevated levels of NO_3^- also in African wildfires[15,54], and here we see increases in NO_3^-/EC during the dry period, although less pronounced when compared to the K^+/EC trend, noting that the latter is more specific for wood burning (Fig. 2). Taken together, we find an imprint on Nairobi air of long-range air mass transport from boreal summer season large-scale African fires, but not to the extent that is seriously altering the air quality.

The source-diagnostic $\Delta^{14}C$ signature in Nairobi BC. The $\Delta^{14}C$ signature is a unique tracer for quantitatively constraining the relative contributions from biomass burning vs fossil combustion to BC, with high precision. Here, we find that BC aerosols in Nairobi were highly depleted in ^{14}C throughout the study period ($\Delta^{14}C = -840 \pm 34‰$; Fig. 4). Unlike biomass ($\Delta^{14}C_{biomass} = +57 \pm 52‰$), fossil fuels are radiocarbon dead ($\Delta^{14}C_{fossil} = -1000‰$). Therefore, the highly depleted $\Delta^{14}C$ values indicate a dominant contribution from fossil fuel combustion. The $\Delta^{14}C$ signature remained comparably constant throughout, with no distinct seasonal or temporal trend, and implying a minimal shift in BC source strength (Fig. 4).

A high influence of fossil emissions on BC levels, and Nairobi's air quality in general, is hereby realised. The year-round averaged fossil fraction accounted for 85 ± 3% of the BC emissions (Eq. 1). This translates to an annual average of $3.4 \pm 1.1\ \mu g\ m^{-3}$ of BC from fossil fuel combustion emissions and $0.6 \pm 0.1\ \mu g\ m^{-3}$ from biomass burning. Similar to BC concentrations, but different from biomass burning markers such as K^+/BC, there was no clear seasonality in the fossil and biomass burning fractions and their respective concentrations (Fig. 4). Therefore, the BC sources were predominantly local, and constant through the year, with minimal influence from regional biomass burning episodes. The differences in the seasonal trends between ^{14}C-derived biomass BC concentrations and K^+/BC is explained by the large variability in biomass burning emission factors for different components (e.g. K^+ is mainly a marker of wood-burning, while much of BC in Africa is also from burned grasses), but is also by the differences in atmospheric processing and atmospheric transport[15]. The elevated fossil fuel combustion contributions to BC found here is in qualitative agreement with previous conclusions for Nairobi[18,22,55]. However, while the present isotope-based study specifically source apportions BC, previous studies used different

chemical tracers to apportion $PM_{2.5}$, making the approaches and results largely complementary.

The high fossil contribution to BC reported here is consistent with the lack of an effective transport policy in Nairobi, leading to heavy traffic congestion[16,55,56]. Nairobi city is estimated to accommodate over a third of the 3.1 million registered vehicles in Kenya, while 68% of the fuel imports are consumed in the transport sector[16,57]. The fleet's fuel economy, consisting mainly of second-hand imported vehicles and two-wheelers, is two to three times lower than in developed countries[56,58–61]. Besides, higher altitude in Nairobi (1690 m asl.) could increase vehicular emissions due to lower absolute O_2 levels, which give a less efficient combustion[62,63]. The industry and commerce sector consumes 16% of the petroleum fuels, while coal contributes under a percentage of Kenya's energy mix[57]. Meanwhile, in informal settlements and low-income neighbourhoods, the use of kerosene cookstoves and biomass fuels e.g. charcoal—we find a background biomass signature—is still prevalent and a potential BC source[30,64].

Similar to Nairobi, urban sites around the world generally exhibit a higher fraction of BC from fossil origins (SI Table S3). ^{14}C-derived fossil contributions accounting for over 75% of BC are reported in North American[65,66] and European Cities[67–70], while the actual BC concentrations in these cities are lower than in SSA cities. East Asian cities also have elevated fossil contributions and BC concentrations in the same range as Nairobi, but are much larger in size and activity levels[25,41,71,72]. For some South Asian cities, e.g. Delhi and Dhaka, there is a clear seasonal impact from upwind biomass burning activities, as detected by ^{14}C in BC[40,73]. Although we do find elevated levels of biomass burning tracers, e.g. K^+/EC, during periods of regional fires upwind of Nairobi, the signal is not detectable in the ^{14}C-signal in BC, likely reflecting differences in emission factors and atmospheric fate.

Outlook. Air pollution is a major impediment towards resilient and sustainable cities in the SSA region, e.g. challenging the UN Sustainable Developmental Goals. A near-universal measure of air quality is $PM_{2.5}$, with clear health guidelines defined by the WHO[43]. Despite increasing efforts, observational data on the magnitude, composition and sources of $PM_{2.5}$ are still scarce in SSA[6,8,9]. Here, we report that the annual average $PM_{2.5}$ levels in Nairobi are over five times the WHO recommended limits[43]. The overall air quality situation is further compounded by high indoor pollution levels, especially in informal settlements[24,30,64]. Especially, the relative contributions of BC in $PM_{2.5}$ are highly elevated (~15%). Unfortunately, this appears to be a common feature among several SSA cities, that sets the region aside from other continents. While BC is particularly toxic, it is also a strong climate warming forcer of regional climate. Taken together, this suggests that BC should be specifically emphasised when discussing SSA air quality and when designing additional air quality measurement programmes, with potential benefits on climate.

The high fossil contributions to BC in Nairobi reported here most likely reflect traffic emissions, including high-emitting vehicles. The fossil contributions to BC in other SSA cities remains to be investigated, but traffic in SSA overall share the characteristics of Nairobi, making it a prime suspect when it comes to contributions to regional air quality[6,9,56,58,59]. An increasing trend in traffic use over a larger SSA region is consistent with the satellite-based observation of NO_X[54,74].

Overall, rapid urbanisation and population growth in SSA will, if left unregulated, lead to a rapidly deteriorating air pollution problem[23,75]. The region's carbonaceous aerosol emissions are expected to contribute to 50% of the global emissions by 2030[7,76]. Even for urban Nairobi, the contribution from carbonaceous aerosols to $PM_{2.5}$ is major (64 ± 11%), while for background sites it is even larger[15]. Beyond human respiratory health, such emissions may interfere with the regional climate in unfavourable ways[29]. For instance, interference with the African monsoon system will have major consequences for floods, droughts, and freshwater supply, negatively affecting the region's largely agrarian economies[77,78].

Overall, this study stresses the importance of regional initiatives to combat air pollution and BC emissions in particular. Investing in an efficient public transport system, promoting non-motorised transport, and enforcing fuel and emission standards appear to be, although socio-economically challenging, feasible strategies to counter the current trajectory.

Methods

$PM_{2.5}$ Sampling. The sampling site was located on the rooftop of one of the University of Nairobi buildings (1.279°S, 36.817°E; 1690 m above sea level; 17 m above ground level), in a park-like environment near the Nairobi city centre. Nairobi—Kenya's capital city—hosts around 4.4 million residents, with a daytime population of over six million people[79]. Based on a compilation of literature studies, the 'Nairobi City County Air Quality Action Plan (2019–2023)' identified traffic, refuse to burn, and industrial emissions as key pollutant sources in the city[16]. However, the sampling site experienced neither direct influences from emission sources such as industries, traffic hotspots and dumpsite/refuse to burn, nor obstruction to the free flow of air masses. The surrounding roads usually experience low vehicle density, with restricted use for public service vehicles - locally known as 'Matatus' - and heavy trucks. Therefore, the site was considered representative of the background air quality in the city, as previously described[18,80].

A high-volume sampler (model DH-77, Digitel A.G., Switzerland; flowrate of ~30 $m^3\,h^{-1}$) with $PM_{2.5}$ inlet was installed and used to collect 24-h filter samples every 6th day—to ensure all days of the week are represented—on prebaked (450 °C for 6 h) quartz fibre filters (Millipore, 150 mm diameter). Monthly field blanks were also collected by loading the filter into the sampler without starting the pump. In total, 66 filter samples were collected between March 2014 and February 2015.

Concentration measurements. $PM_{2.5}$ mass concentrations were determined gravimetrically by dividing mass loading (difference in filter mass before and after sampling) by sampled air volume. The mass determination was performed in a specially-constructed temperature- and humidity-controlled room ($T = 20 \pm 1$ °C, Rh = 40 ± 5%). Before weighing, filters were equilibrated for 24 h.

Water-soluble inorganic ions (WSII) were analyzed using the Dionex Aquion ion chromatography instrument (Thermo Finnigan LLC), applying a previously described analysis protocol[53]. The aerosol BC (quantified as mass-based equivalent-elemental carbon, EC) and organic carbon (OC) concentrations were measured with a thermal-optical transmission (TOT) analyzer (Sunset Laboratory, Tigard, Oregon) using the NIOSH 5040 protocol[81]. The instrument response was calibrated using a sucrose standard, while the analytical precision was ascertained using analyses traceable to the NIST Urban Dust Standard Reference Material, SRM-8785. The OC values were blank corrected by subtracting an average of the field blanks (0.9 ± 0.3 μg cm^{-2}; equivalent to 0.02 μg m^{-3}). No BC was detected in the field blanks ($n = 13$). Analysis of triplicates was conducted to check measurement precision and sample homogeneity, and showed a mean relative standard deviation of 3% for OC and 2% for EC, well within the instrumental error at 5 and 6%, respectively. For WSII, the average relative s.d. is <5% for all measured ions.

$\Delta^{14}C$ source apportionment. Roughly every second sample (excluding blanks) for the year-round study period was selected for isolation and cryo-trapping of BC ($n = 28$) for ^{14}C analysis, using a modified Sunset TOT instrument and a previously described protocol[25,26]. In brief, the BC deposited on the filter is thermally separated from OC and combusted into CO_2. The produced CO_2 is then diverted and purified online through silver wool and magnesium perchlorate traps to remove halogens and moisture, respectively. Subsequently, the CO_2 is cryo-trapped in liquid N_2 and flame sealed in glass ampoules. Ag and CuO were preadded into the glass ampoules, and combusted for 6 h at 400 °C, to remove gas impurities that may interfere with isotopic analyses[26]. The trapped CO_2 samples were then analysed for $\Delta^{14}C$ signatures using an accelerator mass spectrometer (AMS), at the Radiocarbon Laboratory at Uppsala University, Sweden.

To quantify the fractional contributions from biomass burning ($f_{biomass}$) versus fossil fuel combustion ($f_{fossil} = 1 - f_{biomass}$), we applied the isotopic mass balance equation:

$$\Delta^{14}C_{sample} = f_{biomass} \cdot \Delta^{14}C_{biomass} + (1 - f_{biomass}) \cdot \Delta^{14}C_{fossil} \quad (1)$$

where $\Delta^{14}C_{sample}$ represents the radiocarbon signature of the sample, and $\Delta^{14}C_{fossil}$ is

the fossil signature at −1000‰. The $\Delta^{14}C_{biomass}$ endmember may vary between +20‰ and +225‰, reflecting the $\Delta^{14}C$ signature for atmospheric CO_2, as influenced by 1960s nuclear bomb tests, fossil CO_2 emissions, and global carbon recycling. As such, annual plants carry the ambient $\Delta^{14}C$ signatures (+20‰ for 2014/2015), while more long-lived organic matter (e.g. trees) may be more enriched in ^{14}C[36,82]. For this study, a regionally parametrised SSA biomass endmember for 2015, $\Delta^{14}C_{biomass} = +57 \pm 52$‰, was used[15].

Pyrolized carbon, formed during combustion of OC in the helium phase of the NIOSH 5040 protocol, may be inadvertently trapped with BC fraction. Here we estimate that such phenomena may potentially shift the $\Delta^{14}C$ of BC by a maximum of 30‰, which is within the uncertainty margin of the isotope measurements (SI Note S1).

Meteorology, air mass back trajectories and satellite products. Local meteorology parameters (e.g. wind speed and direction, temperature and rainfall) were obtained from the meteorological station at Jomo Kenyatta International airport (JKIA) in Nairobi and complemented with meteorological parameters retrieved from the Global Data Assimilation System (GDAS). To investigate potential influence from other geographical locations on air pollution in Nairobi, 5-days air mass back trajectories (BT) were computed every 6 hours, with an arrival height of 100 m above ground level (1890 m a.s.l). For BT analysis, the NOAA Hybrid Single-Particle Lagrangian Integrated Trajectory Model (HYSPLIT, version 4) and GDAS (1° × 1°) archived meteorological datasets were used[83]. Remote sensing fire-spot detections were retrieved from the NASA Fire Information for Resource Management Services (FIRMS) database, based on retrievals from the Moderate Resolution Imaging Spectroradiometer (MODIS) satellite product[84].

Data availability

Concentrations of $PM_{2.5}$, carbonaceous aerosols, inorganic ions and radiocarbon data for BC for the present study in Nairobi is available at the Bolin Centre Database (bolin.su.se/data/) with https://doi.org/10.17043/andersson-2022-nairobi-1.

Received: 1 July 2021; Accepted: 1 March 2022;
Published online: 01 April 2022

References

1. WHO. *Ambient Air Pollution: A Global Assessment of Exposure and Burden of Disease* (World Health Organization, 2016).
2. Lelieveld, J. et al. Loss of life expectancy from air pollution compared to other risk factors: a worldwide perspective. *Cardiovasc. Res.* **116**, 1910–1917 (2020).
3. WHO Regional Office for Africa. *The Health of the People. African Regional Health Report* 2014 (WHO Regional Office for Africa, 2014).
4. Bauer, S. E., Im, U., Mezuman, K. & Gao, C. Y. Desert dust, industrialization, and agricultural fires: health impacts of outdoor air pollution in Africa. *J. Geophys. Res. Atmos.* **124**, 4104–4120 (2019).
5. Burnett, R. et al. Global estimates of mortality associated with longterm exposure to outdoor fine particulate matter. *Proc. Natl. Acad. Sci. USA* **115**, 9592–9597 (2018).
6. Amegah, A. K. & Agyei-Mensah, S. Urban air pollution in Sub-Saharan Africa: time for action. *Environ. Pollut.* **220**, 738–743 (2017).
7. Liousse, C., Assamoi, E., Criqui, P., Granier, C. & Rosset, R. Explosive growth in African combustion emissions from 2005 to 2030. *Environ. Res. Lett.* **9**, 035003 (2014).
8. Petkova, E. P., Jack, D. W., Volavka-Close, N. H. & Kinney, P. L. Particulate matter pollution in African cities. *Air Qual. Atmos. Heal.* **6**, 603–614 (2013).
9. Agbo, K. E. et al. A review on ambient and indoor air pollution status in Africa. *Atmos. Pollut. Res.* **12**, 243–260 (2021).
10. UN Department of Economic and Social Affairs. *World Urbanization Prospects: The 2018 Revision* (UN, 2018).
11. Awe, Y. et al. Filling the gaps: improving measurement of ambient air quality in low and middle income countries. http://pubdocs.worldbank.org/en/425951511369561703/Filling-the-Gaps-White-Paper-Discussion-Draft-November-2017.pdf (2017).
12. DeWitt, H. L. et al. Seasonal and diurnal variability in O3, black carbon, and CO measured at the Rwanda Climate Observatory. *Atmos. Chem. Phys.* **19**, 2063–2078 (2019).
13. Kulmala, M. Build a global Earth observatory. *Nature* **553**, 21–23 (2018).
14. López-Ballesteros, A. et al. Towards a feasible and representative pan-African research infrastructure network for GHG observations. *Environ. Res. Lett.* **13**, 085003 (2018).
15. Andersson, A. et al. Seasonal source variability of carbonaceous aerosols at the Rwanda Climate Observatory. *Atmos. Chem. Phys.* **20**, 4561–4573 (2020).
16. Nairobi City County. *Nairobi City County Air Quality Action Plan* (2019-2023). https://www.eci-africa.org/wp-content/uploads/2019/05/Nairobi-Air-Quality-Action-Plan_Final_ECI_31.12.2018.pdf (2019).
17. Antonel, J. & Chowdhury, Z. Measuring ambient particulate matter in three cities in Cameroon, Africa. *Atmos. Environ.* **95**, 344–354 (2014).
18. Gaita, S. M., Boman, J., Gatari, M. J., Pettersson, J. B. C. & Janhäll, S. Source apportionment and seasonal variation of PM2.5 in a sub-Saharan African city: Nairobi, Kenya. *Atmos. Chem. Phys.* **14**, 9977–9991 (2014).
19. Zeng, L. et al. Comparison of PM2.5 pollution between an African city and an Asian metropolis. *Sci. Total Environ.* **696**, 134069 (2019).
20. Zhou, Z. et al. Chemical composition and sources of particle pollution in affluent and poor neighborhoods of Accra, Ghana. *Environ. Res. Lett.* **8**, 044025 (2013).
21. Mkoma, S. L., Maenhaut, W., Chi, X., Wang, W. & Raes, N. Characterisation of PM10 atmospheric aerosols for the wet season 2005 at two sites in East Africa. *Atmos. Environ.* **43**, 631–639 (2009).
22. Gatari, M. J. et al. High airborne black carbon concentrations measured near roadways in Nairobi. *Kenya. Transp. Res. Part D* **68**, 99–109 (2019).
23. Keita, S. et al. African anthropogenic emissions inventory for gases and particles from 1990 to 2015. *Earth Syst. Sci. Data* **13**, 1–29 (2020).
24. Egondi, T., Muindi, K., Kyobutungi, C., Gatari, M. & Rocklöv, J. Measuring exposure levels of inhalable airborne particles (PM2.5) in two socially deprived areas of Nairobi, Kenya. *Environ. Res.* **148**, 500–506 (2016).
25. Chen, B. et al. Source forensics of black carbon aerosols from China. *Environ. Sci. Technol.* **47**, 9102–9108 (2013).
26. Andersson, A. et al. Regionally-varying combustion sources of the january 2013 severe haze events over eastern China. *Environ. Sci. Technol.* **49**, 2038–2043 (2015).
27. Janssen, N. A. et al. *Health Effects of Black Carbon* (WHO, 2012).
28. Bond, T. C. et al. Bounding the role of black carbon in the climate system: a scientific assessment. *J. Geophys. Res. Atmos.* **118**, 5380–5552 (2013).
29. Boucher, O. et al. in *Climate Change 2013 the Physical Science Basis: Working Group I Contribution to the Fifth Assessment Report of the Intergovernmental Panel on Climate Change* (eds Stocker, T. F. et al.) Ch. 7 (Cambridge Univ. Press, 2013).
30. Bockarie, A. S., Marais, E. A. & Mackenzie, A. R. Air pollution and climate forcing of the charcoal industry in Africa. *Environ. Sci. Technol.* **54**, 13429–13438 (2020).
31. Zhao, Y., Nielsen, C. P., Lei, Y., McElroy, M. B. & Hao, J. Quantifying the uncertainties of a bottom-up emission inventory of anthropogenic atmospheric pollutants in China. *Atmos. Chem. Phys.* **11**, 2295–2308 (2011).
32. Dasari, S. et al. Source quantification of South Asian black carbon aerosols with isotopes and modeling. *Environ. Sci. Technol.* **54**, 11771–11779 (2020).
33. Winiger, P., Andersson, A., Eckhardt, S., Stohl, A. & Gustafsson, O. The sources of atmospheric black carbon at a European gateway to the Arctic. *Nat. Commun.* **7**, 12776 (2016).
34. Akagi, S. K. et al. Emission factors for open and domestic biomass burning for use in atmospheric models. *Atmos. Chem. Phys.* **11**, 4039–4072 (2011).
35. Gustafsson, Ö. et al. Brown clouds over South Asia: biomass or fossil fuel combustion? *Science.* **323**, 495–498 (2009).
36. Graven, H. D., Guilderson, T. P. & Keeling, R. F. Observations of radiocarbon in CO 2 at seven global sampling sites in the Scripps flask network: analysis of spatial gradients and seasonal cycles. *J. Geophys. Res.* **117**, D02303 (2012).
37. Huang, L. et al. Stable isotope measurements of carbon fractions (OC / EC) in airborne particulate: a new dimension for source characterization and apportionment. *Atmos. Environ.* **40**, 2690–2705 (2006).
38. Winiger, P. et al. Source apportionment of circum-Arctic atmospheric black carbon from isotopes and modeling. *Sci. Adv.* **5**, eaau8052 (2019).
39. Budhavant, K. et al. Radiocarbon-based source apportionment of elemental carbon aerosols at two South Asian receptor observatories over a full annual cycle. *Environ. Res. Lett.* **10**, 064004 (2015).
40. Bikkina, S. et al. Air quality in megacity Delhi affected by countryside biomass burning. *Nat. Sustain.* **2**, 200–205 (2019).
41. Fang, W. et al. Dual-isotope constraints on seasonally resolved source fingerprinting of black carbon aerosols in sites of the four emission hot spot regions of China. *J. Geophys. Res. Atmos.* **123**, 735–11,747 (2018).
42. Henne, S., Junkermann, W., Kariuki, J. M., Aseyo, J. & Klausen, J. Mount Kenya global atmosphere watch station (MKN): installation and meteorological characterization. *J. Appl. Meteorol. Climatol.* **47**, 2946–2962 (2008).
43. WHO. *WHO Global Air Quality Guidelines. Particulate Matter (PM2.5 and PM10), Ozone, Nitrogen Dioxide, Sulfur Dioxide and Carbon Monoxide* (WHO, 2021).
44. El-Zanan, H. S., Zielinska, B., Mazzoleni, L. R. & Hansen, D. A. Analytical determination of the aerosol organic mass-to-organic carbon ratio. *J. Air Waste Manag. Assoc.* **59**, 58–69 (2009).

45. Silvern, R. F. et al. Inconsistency of ammonium-sulfate aerosol ratios with thermodynamic models in the eastern US: A possible role of organic aerosol. *Atmos. Chem. Phys.* **17**, 5107–5118 (2017).
46. Gatari, M. J., Boman, J. & Wagner, A. Characterization of aerosol particles at an industrial background site in Nairobi, Kenya. *X-Ray Spectrom.* **38**, 37–44 (2009).
47. Ngo, N. S. et al. Occupational exposure to roadway emissions and inside informal settlements in sub-Saharan Africa: A pilot study in Nairobi, Kenya. *Atmos. Environ.* **111**, 179–184 (2015).
48. Shilenje, Z. et al. Roadside air pollutants along elected roads in Nairobi City, Kenya. *J. Geol. Geophys.* **5,** 1–10 (2016).
49. Nairobi City County. *Nairobi Air Quality Action Plan* (UN, 2019).
50. Mkoma, S. L., Chi, X. & Maenhaut, W. Characteristics of carbonaceous aerosols in ambient PM10 and PM2.5 particles in Dar es Salaam, Tanzania. *Sci. Total Environ.* **408**, 1308–1314 (2010).
51. Djossou, J. et al. Mass concentration, optical depth and carbon composition of particulate matter in the major southern West African cities of Cotonou (Benin) and Abidjan (Côte d'Ivoire). *Atmos. Chem. Phys.* **18**, 6275–6291 (2018).
52. Huang, R. J. et al. High secondary aerosol contribution to particulate pollution during haze events in China. *Nature* **514**, 218–222 (2015).
53. Dasari, S. et al. Photochemical degradation affects the light absorption of water-soluble brown carbon in the South Asian outflow. *Sci. Adv.* **5**, 1–11 (2019).
54. Hickman, J. E. et al. Reductions in NO2 burden over north equatorial Africa from decline in biomass burning in spite of growing fossil fuel use, 2005 to 2017. *Proc. Natl Acad. Sci. USA* **118**, (2021).
55. Kinney, P. L. et al. Traffic impacts on PM2.5 air quality in Nairobi, Kenya. *Environ. Sci. Policy* **14**, 369–378 (2012).
56. Mbandi, A. M. et al. Estimating on-road vehicle fuel economy in Africa: a case study based on an urban transport survey in Nairobi, Kenya. *Energies* **12**, 6–8 (2019).
57. Kenya National Bureau of Statistics. *Economic Survey 2018* (Kenya National Bureau of Statistics, 2018).
58. Doumbia, M. et al. Emissions from the road traffic of West African cities: assessment of vehicle fleet and fuel consumption. *Energies* **11**, 1–16 (2018).
59. Adiang, C. M., Monkam, D., Njeugna, E. & Gokhale, S. Projecting impacts of two-wheelers on urban air quality of Douala, Cameroon. *Transp. Res. Part D Transp. Environ.* **52**, 49–63 (2017).
60. Keita, S. et al. Particle and VOC emission factor measurements for anthropogenic sources in West Africa. *Atmos. Chem. Phys.* **18**, 7691–7708 (2018).
61. Marais, E. A. & Wiedinmyer, C. Air quality impact of diffuse and inefficient combustion emissions in Africa (DICE-Africa). *Environ. Sci. Technol.* **50**, 10739–10745 (2016).
62. Fang, L., Lou, D., Hu, Z. & Tan, P. The emission characteristics of a diesel engine during start-up process at different altitudes. *Energies* **12**, 3556 (2019).
63. Ghazikhani, M., Ebrahim Feyz, M., Mahian, O. & Sabazadeh, A. Effects of altitude on the soot emission and fuel consumption of a light-duty diesel engine. *Transport* **28**, 130–139 (2013).
64. Mutahi, A. W., Borgese, L., Marchesi, C., Gatari, M. J. & Depero, L. E. Indoor and outdoor air quality for sustainable life: a case study of rural and urban settlements in poor neighbourhoods in kenya. *Sustainability* **13**, 1–18 (2021).
65. Mouteva, G. O. et al. Using radiocarbon to constrain black and organic carbon aerosol sources in Salt Lake City. *J. Geophys. Res. Atmos.* **122**, 9843–9857 (2017).
66. Yoon, S., Fairley, D., Barrett, T. E. & Sheesley, R. J. Biomass and fossil fuel combustion contributions to elemental carbon across the San Francisco Bay Area. *Atmos. Environ.* **195**, 229–242 (2018).
67. Bernardoni, V. et al. Radiocarbon analysis on organic and elemental carbon in aerosol samples and source apportionment at an urban site in Northern Italy. *J. Aerosol Sci.* **56**, 88–99 (2013).
68. Heal, M. R. et al. Application of 14C analyses to source apportionment of carbonaceous PM2.5 in the UK. *Atmos. Environ.* **45**, 2341–2348 (2011).
69. Minguillón, M. C. et al. Fossil versus contemporary sources of fine elemental and organic carbonaceous particulate matter during the DAURE campaign in Northeast Spain. *Atmos. Chem. Phys.* **11**, 12067–12084 (2011).
70. Szidat, S. et al. Contributions of fossil fuel, biomass-burning, and biogenic emissions to carbonaceous aerosols in Zurich as traced by 14C. *J. Geophys. Res. Atmos.* **111**, 1–12 (2006).
71. Zhang, Y. L. et al. Fossil vs. non-fossil sources of fine carbonaceous aerosols in four Chinese cities during the extreme winter haze episode of 2013. *Atmos. Chem. Phys.* **15**, 1299–1312 (2015).
72. Yamamoto, N. et al. Comparison of carbonaceous aerosols in Tokyo before and after implementation of diesel exhaust restrictions. *Environ. Sci. Technol.* **41**, 6357–6362 (2007).
73. Salam, A. et al. Wintertime air quality in Megacity Dhaka, Bangladesh strongly affected by influx of black carbon aerosols from regional biomass burning. *Environ. Sci. Technol.* 55, 12243–12249 (2021).
74. Song, W. et al. Important contributions of non-fossil fuel nitrogen oxides emissions. *Nat. Commun.* **12**, 1–7 (2021).
75. UNDP. *2018 Africa Sustainable Development Report: Towards a Transformed and Resilient Continent* (UNECA, 2018).
76. Ramo, R. et al. African burned area and fire carbon emissions are strongly impacted by small fires undetected by coarse resolution satellite data. *Proc. Natl Acad. Sci. USA* **118**, 1–7 (2021).
77. Niang, I. et al. *Climate Change 2014 – Impacts, Adaptation and Vulnerability-Working Group II Contribution to the IPCC Fifth Assessment Report*. Ch.22 (Cambridge Univ. Press, 2014).
78. Hodnebrog, O., Myhre, G., Forster, P. M., Sillmann, J. & Samset, B. H. Local biomass burning is a dominant cause of the observed precipitation reduction in southern Africa. *Nat. Commun.* **7**, 11236 (2016).
79. Kenya National Bureau of Statistics. *Kenya Population and Housing Census Volume 1: Population by County and sub-County*. (Kenya National Bureau of Statistics, 2019).
80. Pope, F. D., Gatari, M., Ng, D., Poynter, A. & Blake, R. Airborne particulate matter monitoring in Kenya using calibrated low-cost sensors. *Atmos. Chem. Phys.* **18**, 15403–15418 (2018).
81. Birch, M. E. & Cary, R. A. Elemental carbon-based method for monitoring occupational exposures to particulate diesel exhaust. *Aerosol Sci. Technol.* **25**, 221–241 (1996).
82. Turnbull, J. C. et al. Sixty years of radiocarbon dioxide measurements at Wellington, New Zealand: 1954 – 2014. *Atmos. Chem. Phys.* **17**, 14771–14784 (2017).
83. Stein, A. F. et al. Noaa's hysplit atmospheric transport and dispersion modeling system. *Bull. Am. Meteorol. Soc.* **96**, 2059–2077 (2015).
84. Justice, C. O. et al. The MODIS fire products. *Remote Sens. Environ.* **83**, 244–262 (2002).

Acknowledgements

This work is supported by research grants from the Swedish Research Council (VR contracts nos. 2013-114, 2017-05687 and 2020-05384) and the Swedish Research Council for Sustainable Development (FORMAS contract no. 2020-01951). M.J.G. acknowledges the International Science Programme (ISP, Sweden) for capacity and infrastructure support to the Institute of Nuclear Science & Technology (INST), University of Nairobi. We acknowledge the use of data and imagery from LANCE FIRMS, operated by NASA's Earth Science Data and Information System, and HYSPLIT transport and dispersion model and the READY website operated by the NOAA Air Resources Laboratory (http://www.ready.noaa.gov, last access: 17 April 2021).

Author contributions

A.A. conceived and designed the study. L.K. performed sample and data analysis. M.J.G. coordinated the field sampling. Ö.G. established the analytical protocol used. L.K. and A.A. wrote the paper with input from M.J.G. and Ö.G.

Funding

Open access funding provided by Stockholm University.

Competing interests

The authors declare no competing interests.

Additional information

Supplementary information The online version contains supplementary material available at https://doi.org/10.1038/s43247-022-00400-1.

Correspondence and requests for materials should be addressed to August Andersson.

Peer review information *Communications Earth & Environment* thanks Abdus Salam and the other, anonymous, reviewer(s) for their contribution to the peer review of this work. Primary Handling Editors: Yinon Rudich, Clare Davis and Heike Langenberg. Peer reviewer reports are available.

Reprints and permission information is available at http://www.nature.com/reprints

Publisher's note Springer Nature remains neutral with regard to jurisdictional claims in published maps and institutional affiliations.

Open Access This article is licensed under a Creative Commons Attribution 4.0 International License, which permits use, sharing, adaptation, distribution and reproduction in any medium or format, as long as you give appropriate credit to the original author(s) and the source, provide a link to the Creative Commons license, and indicate if changes were made. The images or other third party material in this article are included in the article's Creative Commons license, unless indicated otherwise in a credit line to the material. If material is not included in the article's Creative Commons license and your intended use is not permitted by statutory regulation or exceeds the permitted use, you will need to obtain permission directly from the copyright holder. To view a copy of this license, visit http://creativecommons.org/licenses/by/4.0/.

© The Author(s) 2022